Immunity
Article

Toll-like Receptor 4 Is a Sensor for Autophagy Associated with Innate Immunity

Yi Xu,[1] Chinnaswamy Jagannath,[2] Xian-De Liu,[1] Amir Sharafkhaneh,[1] Katarzyna E. Kolodziejska,[1] and N. Tony Eissa[1,*]
[1] Department of Medicine, Baylor College of Medicine, Houston, TX 77030, USA
[2] Department of Pathology and Laboratory of Medicine, University of Texas Health Sciences Center, Houston, TX 77030, USA
*Correspondence: teissa@bcm.edu
DOI 10.1016/j.immuni.2007.05.022

SUMMARY

Autophagy has recently been shown to be an important component of the innate immune response. The signaling pathways leading to activation of autophagy in innate immunity are not known. Here we showed that Toll-like receptor 4 (TLR4) served as a previously unrecognized environmental sensor for autophagy. Autophagy was induced by lipopolysaccharide (LPS) in primary human macrophages and in the murine macrophage RAW264.7 cell line. We defined a new molecular pathway in which LPS-induced autophagy was regulated through a Toll-interleukin-1 receptor domain-containing adaptor-inducing interferon-β (TRIF)-dependent, myeloid differentiation factor 88 (MyD88)-independent TLR4 signaling pathway. Receptor-interacting protein (RIP1) and p38 mitogen-activated protein kinase were downstream components of this pathway. This signaling pathway did not affect cell viability, indicating that it is distinct from the autophagic death signaling pathway. We further showed that LPS-induced autophagy could enhance mycobacterial colocalization with the autophagosomes. This study links two ancient processes, autophagy and innate immunity, together through a shared signaling pathway.

INTRODUCTION

Autophagy is a highly evolutionarily conserved process in virtually all eukaryotic cells. It involves the sequestration of regions of the cytosol within double-membrane-bound compartments and delivery of the contents to the lysosomes for degradation. Autophagy has been shown to be an important player in many critical biological processes such as cellular response to starvation, cell survival and death, cancer, clearance of inclusion bodies in neurodegenerative diseases, and host defense (Levine and Klionsky, 2004; Levine, 2005). Rapidly accumulating functional evidence has shown that autophagy is a component of innate immunity (Kirkegaard et al., 2004) and is involved in the host defense elimination of bacterial pathogens including group A *Streptococcus* (Nakagawa et al., 2004), *Shigella flexneri* (Ogawa et al., 2005), and *Mycobacterium tuberculosis* (Gutierrez et al., 2004; Singh et al., 2006). The signaling pathways leading to activation of pathogen-induced autophagy remain to be elucidated.

Although the process of autophagy was described decades ago, its genetic components have been only recently identified through extensive studies using yeast genetics (Kirkegaard et al., 2004). Substantial progress has been made in understanding genetic factors contributing to the formation of the autophagic vesicles, but the molecular mechanisms and the signaling pathways leading to induction of autophagy are still enigmatic. Although it has been shown that the signals that contribute to induction of autophagy are mediated by the target of rapamycin (TOR), the phosphatidylinositol 3-kinases (PI3Ks), protein phosphatases, and trimeric G proteins, the upstream signaling events are incompletely understood. Furthermore, whereas it is clear that class III PI3Ks are essential for starvation-induced autophagy, it is not known what signaling pathway mediates pathogen-induced autophagy. In immune cells, Toll-like receptors (TLRs) are charged with microbe detection. These receptors represent a conserved family of innate immune recognition receptors that play key roles in detecting microbes, initiating innate immune responses, and linking innate and adaptive immunity (Takeda and Akira, 2005). Among these stimuli, the cell wall of Gram-negative bacteria constituent lipopolysaccharide (LPS), a potent proinflammatory pathogen-associated molecular pattern, is the ligand for TLR4 receptor. In this study, we showed that TLR4 served as a previously unrecognized environmental sensor for autophagy. Autophagy was regulated through a Toll-interleukin-1 receptor domain-containing adaptor-inducing interferon-β (TRIF)-dependent, myeloid differentiation factor 88 (MyD88)-independent TLR4 signaling pathway. Receptor-interacting protein (RIP1) and p38 mitogen-activated protein kinase (MAPK) were downstream components of this pathway. This signaling pathway did not affect cell viability and was not mediated by c-Jun amino-terminal kinase (JNK), indicating that it is distinct from the autophagic death signaling pathway. We further showed that LPS-induced autophagy could overcome mycobacterial phagosome arrest and force its

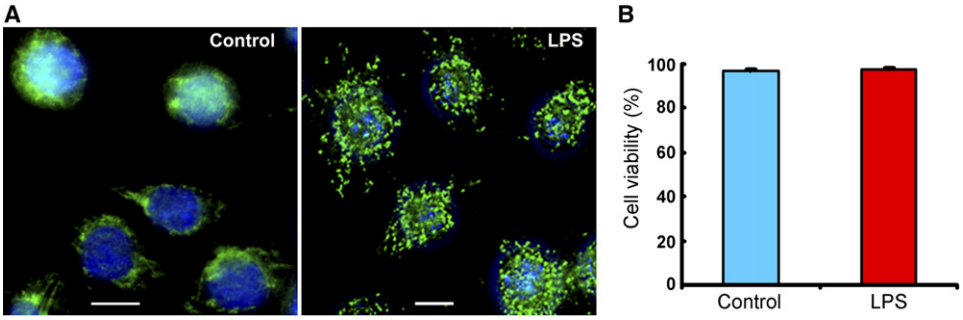

Figure 1. LPS Induces Formation of Autophagosomes

(A) RAW264.7 cells were incubated in the absence or presence of LPS for 16 hr, fixed, stained with DAPI to visualize the nuclei (blue), and immunolabeled with LC3 antibody followed by Alexa Fluor 488-conjugated goat anti-rabbit IgG (green). Representative images are shown. Scale bars = 10 μm. (B) Cell viability analysis of RAW264.7 cells stably expressing GFP-LC3 after incubation in the presence or absence of LPS (100 ng/ml) for 16 hr. Cell viability was determined using a Vi-CELL Cell Viability Analyzer (Beckman Coulter) based on trypan blue reagent (Mean ± SD, n = 4).

colocalization with the autophagosomes. The LPS-induced autophagic signaling pathway further facilitated autophagy vesicle formation by promoting the association of the PI3K VPS34 with the membrane. Furthermore, LPS upregulated LRG47, a guanosine triphosphate (GTP)ase that has been recently shown to be involved in antimycobacterial effects through contribution to autophagy induction (MacMicking et al., 2003; Gutierrez et al., 2004). This study links two ancient processes, autophagy and innate immunity, together through a shared signaling pathway, the Toll-like receptor.

RESULTS

LPS Induces Autophagy in Murine and Human Macrophages

We hypothesized the existence of a potential link between autophagy and LPS-induced innate immune response. To test this hypothesis, we studied autophagy in the murine macrophage cell line RAW264.7 and in primary human alveolar macrophages. Incubation of RAW264.7 cells with LPS (100 ng/ml) led to the redistribution of microtubule-associated protein 1 light chain 3 (LC3, also known as Atg8) from diffuse to punctate staining, typical of autophagosomes (Figure 1A) (Gutierrez et al., 2004; Ogawa et al., 2005). The LPS treatment did not result in a marked effect on cell viability (Figure 1B). We then conducted detailed quantitative analysis of LPS-induced autophagy. LPS induced a significant increase in the percentage of cells expressing autophagosomes (Figure 2A). The increase in type II LC3 was biochemically confirmed by immunoblot analysis with LC3 antibody. LC3 type II, an indicator of autophagosome formation (Nakagawa et al., 2004), was increased in RAW264.7 cells with LPS treatment (Figure 2A, lower panel). Moreover, incubation of RAW264.7 cells stably expressing LC3 fused to green fluorescent protein (GFP-LC3) with LPS also led to the redistribution of GFP-LC3 from diffuse to punctate (Figure 2B) (Gutierrez et al., 2004; Ogawa et al., 2005). GFP-LC3-positive autophagosomes were less numerous compared to autophagosomes detected by immunostaining for endogenous LC3 (compare Figures 2A and 2B). This may be due to inability of GFP-LC3 to be incorporated into all cellular autophagosomes. LPS-induced autophagy was prevented by the coaddition of polymyxin B (PMB), an antibiotic that blocks biological effects of LPS by binding to lipid A, the component of LPS responsible for receptor binding and cellular signaling (Duff and Atkins, 1982; Palsson-McDermott and O'Neill, 2004). Evidence of cellular signaling of LPS was demonstrated through monitoring inducible nitric oxide synthase (iNOS) expression by immunoblot analysis and nitric oxide (NO) production, important downstream products of LPS signaling in RAW264.7 cells (Musial and Eissa, 2001) (Figure 2B, lower panel). Time-course experiments revealed that LPS-induced autophagy could be detected at 8 hr and was maximal at 12–16 hr after LPS stimulation (see Figure S1 in the Supplemental Data available online). The effect of LPS on autophagy was also examined in primary human alveolar macrophages by immunofluorescence. With LPS treatment, 61.8% of cells exhibited autophagosomes compared to 10.3% of control cells (Figure 2C). Furthermore, transmission electron microscopy (EM) was used to examine LPS effect on autophagy. The number of double-membrane vacuoles typical of autophagosomes was markedly increased in RAW264.7 cells treated with LPS compared to control cells (Figure 2D) (Levine and Klionsky, 2004; Ogawa et al., 2005). The above data established the induction of autophagic response in human and murine macrophages after LPS stimulation.

As their maturation proceeds, autophagosomes fuse with endosomal vesicles and acquire lysosome-associated membrane proteins (LAMP1 and LAMP2), thus becoming late autophagosomes that subsequently fuse with lysosomes. Consequently, the colocalization of GFP-LC3 with LAMP1 indicates the presence of late autophagosomes (Kirkegaard et al., 2004). We investigated whether or not LPS induces the formation of mature autophagosomes. In RAW264.7 cells, LPS promoted LAMP1 expression and the maturation of autophagosomes as evidenced by an increase in the colocalization of GFP-LC3 with LAMP1 (data not shown). These results indicate that LPS-induced autophagosomes proceed to mature forms.

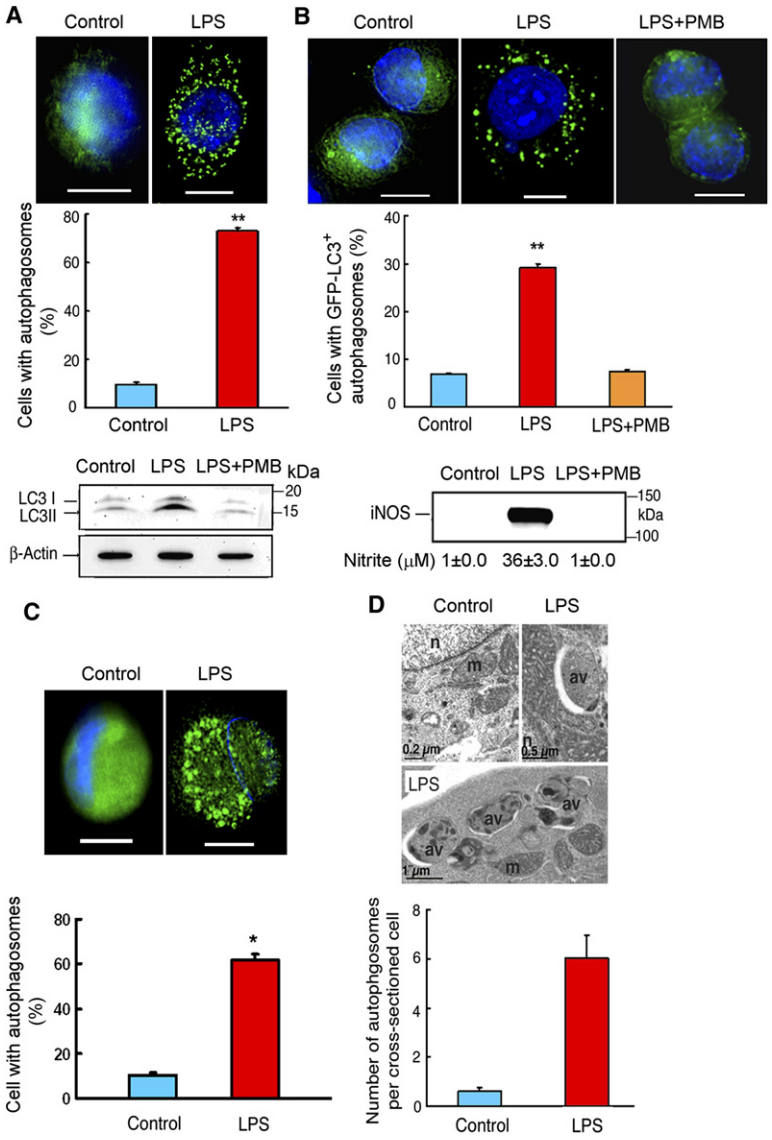

Figure 2. Induction of Autophagy in Primary Human Alveolar Macrophages and Murine Macrophage RAW264.7 Cells by LPS Stimulation

Cells were incubated in the absence (control) or presence of LPS (100 ng/ml) or in the presence of LPS plus PMB (25 μg/ml) for 16 hr.

(A) Upper panel: representative immunofluorescence images with LC3 antibody staining in RAW264.7 cells. Middle panel: quantitation of the percentage of cells with autophagosomes. Lower panel: immunoblot analysis using antibodies against LC3 or β-actin.

(B) GFP-LC3 fluorescence images and quantitation analyses are shown in the upper and middle panels, respectively. Lower panel: immunoblot analysis with iNOS antibody. Activity of iNOS was evaluated by measuring nitrite accumulation in culture media.

(C) Upper panel: representative immunofluorescence images of LC3 antibody staining in primary human alveolar macrophages. Lower panel: quantitation of the percentage of cells with autophagosomes.

(D) Ultrastructural analysis of LPS-induced autophagy by transmission electron microscopy in RAW264.7 cells. av, autophagic vacuole; n, nucleus; m, mitochondria. Graph represents quantitation of the number of autophagosomes per cross-sectioned cell.

Data are mean ± SEM from three (A and B) or two (C and D) independent experiments. *p < 0.05; **p < 0.001 versus control conditions. Scale bars = 10 μm.

TRIF-Dependent TLR4 Signaling Is Required for LPS-Induced Autophagy

LPS exerts multiple cellular effects by inducing signaling through the TLR4 receptor (Beutler and Rietschel, 2003; Palsson-McDermott and O'Neill, 2004). To determine whether or not induction of autophagy by LPS is also mediated through TLR4, a dominant-negative TLR4 mutant and small interfering RNA (siRNA) against TLR4 were used. RAW264.7 cells stably expressing GFP-LC3 were transfected with either vector only or a plasmid expressing a dominant-negative TLR4 mutant. Cells were then subjected to LPS treatment and evaluated for autophagy. LPS-induced autophagy was markedly inhibited in cells transfected with dominant-negative TLR4 compared to cells transfected with vector only (Figure 3A; Figure S2A). In addition, knockdown of TLR4 with specific siRNA completely abrogated the induction of autophagy by LPS (Figure 3B and Figure S2B). These results indicated that LPS-induced autophagy was mediated through signaling by TLR4. Additional experiments were performed using cell line 23 ScCr, which is a bone-marrow-derived macrophage cell line developed from mouse strain C57BL/10ScN with a deletion of the *Tlr4* locus. These mice are naturally deficient in the *Tlr4* gene (Lorenz et al., 2002). These cells could not form autophagosomes in response to LPS (data not shown).

LPS-induced TLR4 signaling pathway uses several adaptors, including MyD88, Toll-interleukin-1 receptor domain-containing adaptor protein (TIRAP), and TRIF. The TLR4 signaling pathway is divided into two categories: MyD88-dependent and MyD88-independent arms (Kawai and Akira, 2005). To determine the role of MyD88-dependent TLR4 signaling in LPS-induced autophagy, we established a stable RAW264.7 cell line that expresses both GFP-LC3 and a dominant-negative MyD88 mutant (MyD88-DN). The percentage of cells with GFP-LC3-positive autophagosomes after LPS treatment in cells expressing both GFP-LC3 and MyD88-DN

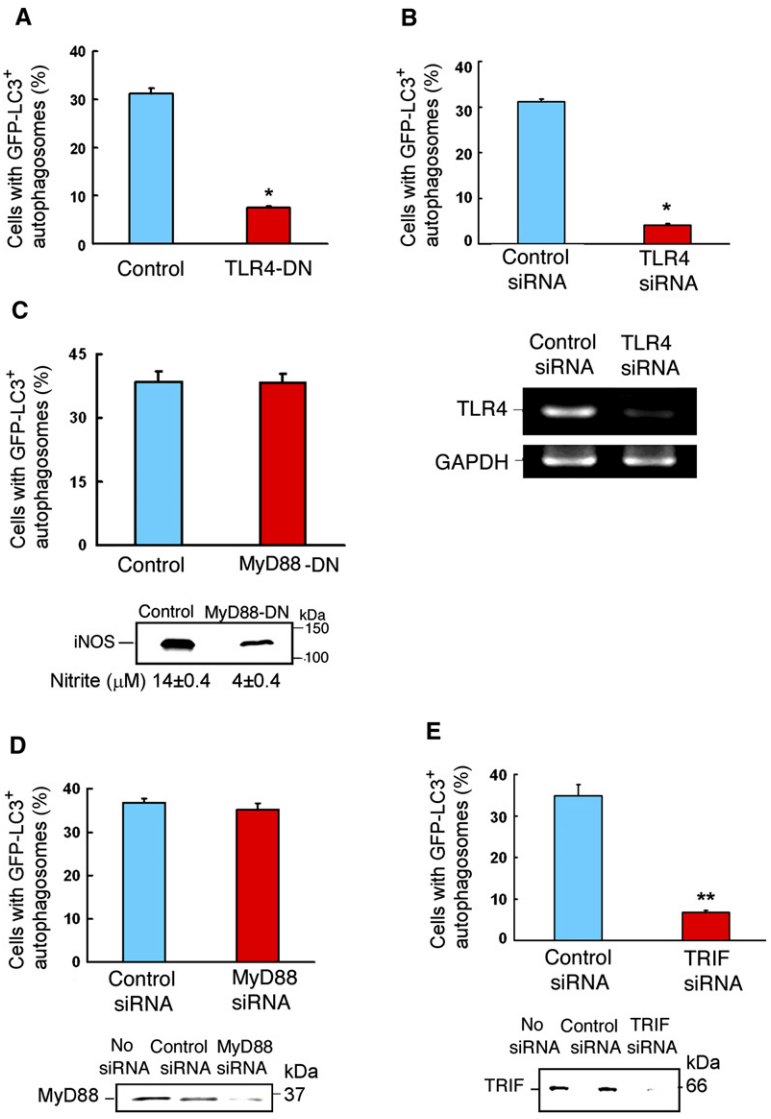

Figure 3. TRIF-Dependent TLR4 Signaling Is Required for LPS-Induced Autophagy

Quantitation analysis of the percentage of cells with GFP-LC3-positive autophagosomes in RAW264.7 cells stably expressing GFP-LC3 after incubation in the presence of LPS (100 ng/ml) for 16 hr. In (A), cells were transfected with vector only or with a plasmid expressing a dominant-negative TLR4 mutant. In (B), (D), and (E), cells were transfected with control siRNA or siRNA specific for TLR4, MyD88, or TRIF, respectively. All transfections were performed for 32 hr prior to LPS treatment. In (C), cells stably expressed both GFP-LC3 and a dominant-negative MyD88 mutant. Lower panel in (B): results of RT-PCR confirming deletion of TLR4 by siRNA. Lower panel in (C): evaluation of iNOS protein expression by immunoblot analysis and iNOS activity by measuring nitrite in culture media. Lower panel in (D): immunoblot analysis of MyD88 in cell lysates. Lower panel in (E): immunoblot analysis of TRIF in cell lysates. Data represent mean ± SEM of three independent experiments. *$p < 0.05$; **$p < 0.001$ versus control conditions.

was similar to that of cells expressing GFP-LC3 only (Figure 3C; Figure S2C). In cells expressing MyD88-DN, inhibition of MyD88-dependent signaling was confirmed by observing the reduction in iNOS expression and NO production by immunoblot analysis and nitrite measurements, respectively (Figure 3C, lower panel). These results suggested that LPS-induced autophagy was not mediated via the MyD88-dependent pathway. We confirmed this finding using siRNA against MyD88. Knockdown of MyD88 by siRNA had no significant effect on LPS-induced autophagy in RAW264.7 cells stably expressing GFP-LC3 (Figure 3D; Figures S2D and S3A). In additional experiments, a peptide inhibitor of TIRAP, another adaptor in the TLR4-MyD88 signaling pathway, failed to block LPS-induced autophagy (data not shown). These data indicated that MyD88 and TIRAP adaptors were not required for LPS-induced autophagy. In contrast to the experiments above, deletion of TRIF by siRNA completely prevented LPS-induced autophagy in RAW264.7 cells stably expressing GFP-LC3 (Figure 3E; Figures S2E and S3B). These results indicated that LPS induced autophagy through a TRIF-dependent TLR4 signaling pathway.

RIP1 and p38 MAPK Are Required for LPS-Induced Autophagy

RIP1 has been characterized as a signaling component of the tumor necrosis factor-induced activation of mitogen-activated protein kinases (Devin et al., 2003). It also participates in TLR3-TRIF-mediated induction of NF-κB activation (Meylan et al., 2004) and in LPS-induced caspase-8-independent cell death in the presence of caspase inhibitors (Holler et al., 2000; Yu et al., 2004; Xu et al., 2006). To examine whether RIP1 mediates LPS-induced autophagy through the TLR4-TRIF pathway, siRNA against RIP1 was used to knock down RIP1 in RAW264.7 cells stably expressing GFP-LC3. Knockdown of RIP1 prevented LPS-induced autophagy (Figure 4A; Figures S2F and S3C), suggesting that RIP1 was required

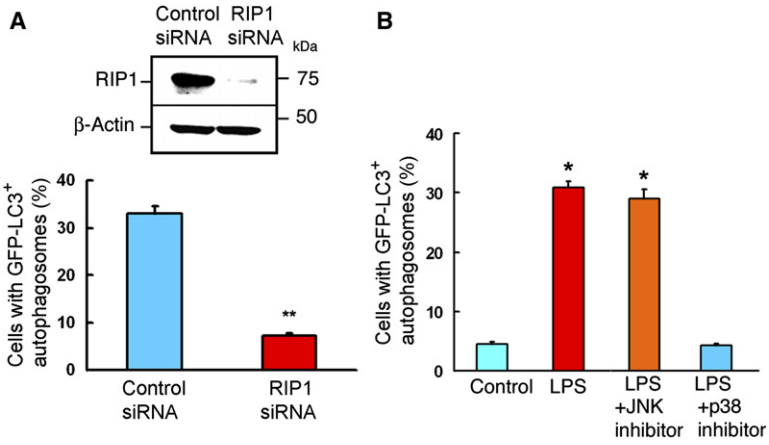

Figure 4. RIP1 and p38 MAPK Are Required for LPS-Induced Autophagy

(A) RAW264.7 cells stably expressing GFP-LC3 were transfected with control siRNA or siRNA specific for RIP1 for 32 hr, followed by LPS treatment (100 ng/ml) for 16 hr. Upper panel: immunoblot analysis of cell lysates with antibodies against RIP1 or β-actin. Lower panel: quantitation analysis of the percentage of cells with GFP-LC3-positive autophagosomes.

(B) RAW264.7 cells stably expressing GFP-LC3 were incubated for 16 hr in the absence (control) or in the presence of LPS+vehicle (DMSO), LPS+JNK inhibitor (20 μM), or LPS+p38 MAPK inhibitor (20 μM). Quantitation of the percentage of cells with GFP-LC3-positive autophagosomes is shown.

Data represent mean ± SEM of three independent experiments. *$p < 0.05$; **$p < 0.001$ versus control conditions.

for this cellular process. Additional siRNA experiments for MyD88, TRIF, and RIP1 were performed using gene-specific scrambled siRNA as a control siRNA (Figure S3). The results were consistent with above data using siRNA against luciferase as a control siRNA.

Previous work suggested a critical role for RIP1 in mediating tumor necrosis factor-induced activation of MAP kinases including JNK and p38 MAPK (Devin et al., 2003). We reasoned that these pathways might also be involved in downstream signaling of the TLR4-TRIF-RIP1 pathway. We examined the effects of inhibition of JNK or p38 MAPK on LPS-induced autophagy in RAW264.7 cells stably expressing GFP-LC3 (Figure 4B; Figure S2G). Inhibition of JNK did not have a marked effect on LPS-induced autophagy. In contrast, p38 MAPK inhibition blocked LPS-induced autophagy (Figure 4B). The effect of p38 MAPK inhibition on LPS-induced autophagy was dose dependent (Figure S4). These data suggested that p38 MAPK was involved in LPS-induced autophagy. Functional assays of JNK and p38 MAPK inhibitors were performed by assaying the phosphorylation of the downstream targets of JNK and p38 MAPK in RAW264.7 cells. JNK activity was assayed by analyzing phosphorylation of c-Jun. p38 MAPK activity was assayed by evaluating phosphorylation of MAP kinase-activated protein kinase 2 (Figure S5).

Inhibition of Class III PI3K Activity Blocks LPS-Induced Autophagy

Inhibition of the class III PI3K by 3-methyladenine (3MA) or wortmannin (Wm) has been shown to inhibit starvation-induced autophagy (Seglen and Gordon 1982; Lum et al., 2005). Our results showed that 3MA (5 mM) or Wm (100 nM) was able to block LPS-induced autophagy as detected by monodansylcadaverine (MDC) staining and GFP-LC3 fluorescence (Figures 5A and 5B).

VPS34 is a class III PI3K that functions in the regulation of autophagy as a catalytic subunit in a complex with beclin 1 and regulatory subunit p150. This complex participates in autophagosome formation through mediating the recruitment of other autophagy proteins to the preautophagosomal membrane (Kihara et al., 2001). To determine whether VPS34 is required for promotion of LPS-induced autophagy, we established a RAW264.7 cell line stably expressing a human dominant-negative VPS34 mutant (Stein et al., 2003). In this cell line, there was no increase in autophagy in response to LPS (Figure 5C), indicating that VPS34 activity was required for the execution of LPS induction of autophagy. The VPS34 complex functions in the promotion of autophagy as a membrane-associated complex (Kihara et al., 2001; Stein et al., 2003). We evaluated the amount of VPS34 associated with the membrane by immunoblot analysis after fractionation of cell lysates into soluble and particulate fractions. In RAW264.7 cells incubated with LPS, there was an increase in the percentage of VPS34 in the particulate fraction (Figure S6), suggesting that LPS promoted the incorporation of VPS34 complex into the membrane.

Colocalization of Mycobacterial Phagosomes with LPS-Induced Autophagosomes

In host phagocytic cells, *Mycobacterium tuberculosis* is known to reside intracellularly in the phagosome and blocks its maturation along the phagosome-lysosome pathway. Induction of autophagy by starvation, rapamycin, or LRG47 expression results in increased colocalization of the mycobacterial phagosomes with the autophagosomes and reduces mycobacterial survival (Gutierrez et al., 2004; Singh et al., 2006). We hypothesized that LPS-induced autophagy can overcome the mycobacterial phagosome block. In RAW264.7 cells infected with *M. tuberculosis*, LPS treatment enhanced colocalization of *M. tuberculosis* with the autophagic vacuoles, compared to infected cells not treated with LPS (Figure 6A). The effects of LPS-induced autophagy on mycobacterial phagosomes were also examined at the ultrastructural level. EM analysis showed that in the absence of LPS, *M. tuberculosis* bacilli were seen in single-membrane-bound phagosomes (Figure 6B, images 1 and 2). In cells treated with LPS, *M. tuberculosis* bacilli were seen inside double-membrane-bound vacuoles typical of autophagosomes

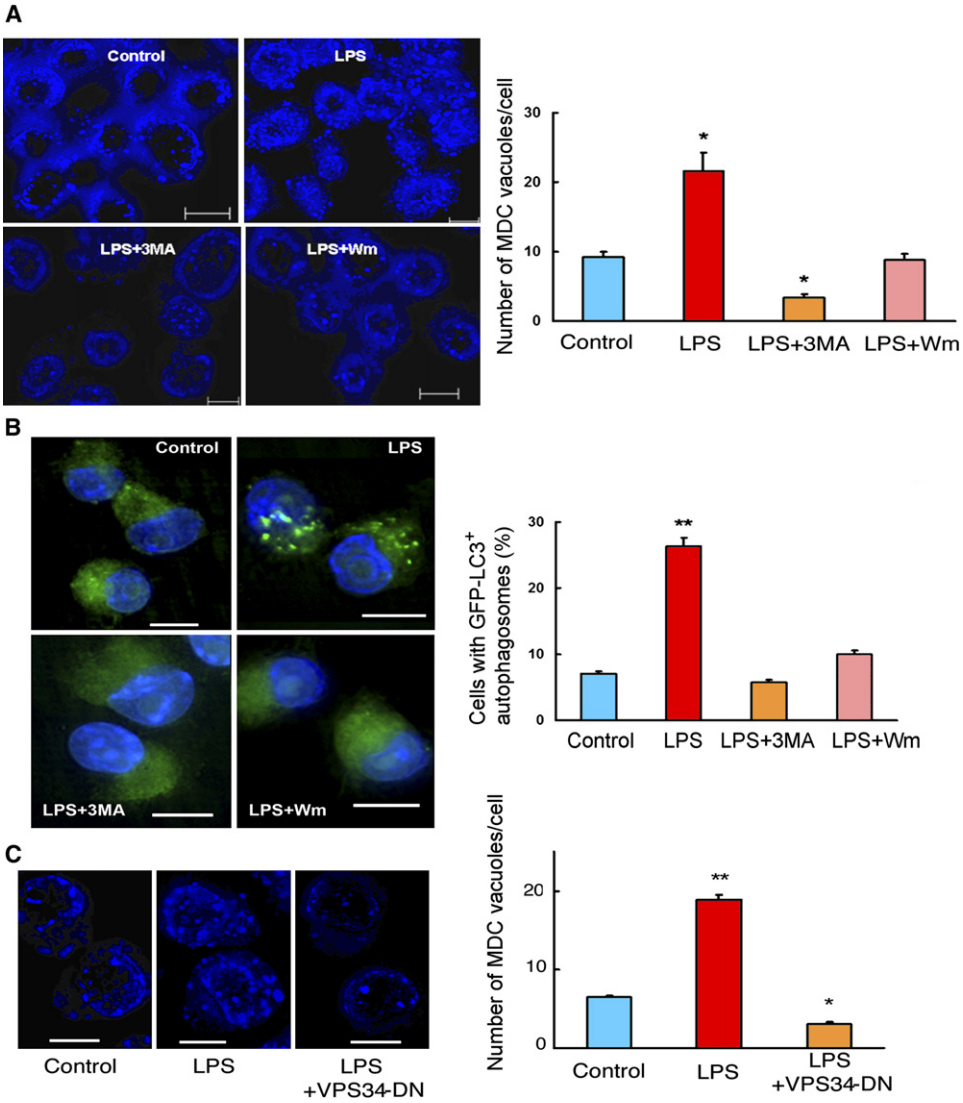

Figure 5. Inhibition of Class III PI3K Activity Blocks LPS-Induced Autophagy

(A) RAW264.7 cells were incubated for 16 hr in the absence (control) or presence of LPS, LPS+3MA (5 mM), or LPS+wortmannin (Wm, 100 nM).

(B) RAW264.7 cells stably expressing GFP-LC3 were subjected to the same conditions as in (A). Cells were fixed and stained with DAPI to visualize the nuclei (blue).

(C) RAW264.7 cells stably expressing a dominant-negative (DN) mutant of VPS34 were incubated with LPS for 16 hr in parallel with RAW264.7 cells incubated with or without LPS. Autophagic vacuoles were stained in fixed cells using monodansylcadaverine (MDC) (blue).

Scale bars = 10 μm. Graphs represent quantitation analysis of the number of MDC-positive autophagosomes per cell (A and C) or the percentage of cells with GFP-LC3-positive autophagosomes (B). Data represent mean ± SEM of three independent experiments. *$p < 0.05$; **$p < 0.001$ versus control conditions.

(Figure 6B, images 3 and 4) (Gutierrez et al., 2004; Ogawa et al., 2005; Lum et al., 2005). Quantitation results showed that 79% of mycobacterial bacilli were found in autophagosomes in LPS-treated cells, compared to only 11% of mycobacterial bacilli residing in autophagosomes in control cells (Figure 6B, lower panel). Potential fusion events of autophagosomes with endosomal structures were seen (Figure 6B, image 5) (Gutierrez et al., 2004). We could also detect autophagosomes with onion-like structures (Figure 6B, image 6), previously reported to occur during autophagy of *M. tuberculosis* and *Shigella* (Gutierrez et al., 2004; Ogawa et al., 2005). These data indicated that LPS-induced autophagy promoted the colocalization of mycobacterial phagosomes with the autophagosomes.

We then tested whether p38 MAPK inhibition could block LPS-induced colocalization of *M. tuberculosis* with autophagosomes. RAW264.7 cells stably expressing GFP-LC3 were infected with *M. tuberculosis* expressing red fluorescent protein 1 hr prior to incubation for 16 hr in the absence of LPS or in the presence of LPS plus vehicle (DMSO) or LPS plus p38 MAPK inhibitor (Figure 7). LPS treatment resulted in a significant increase in

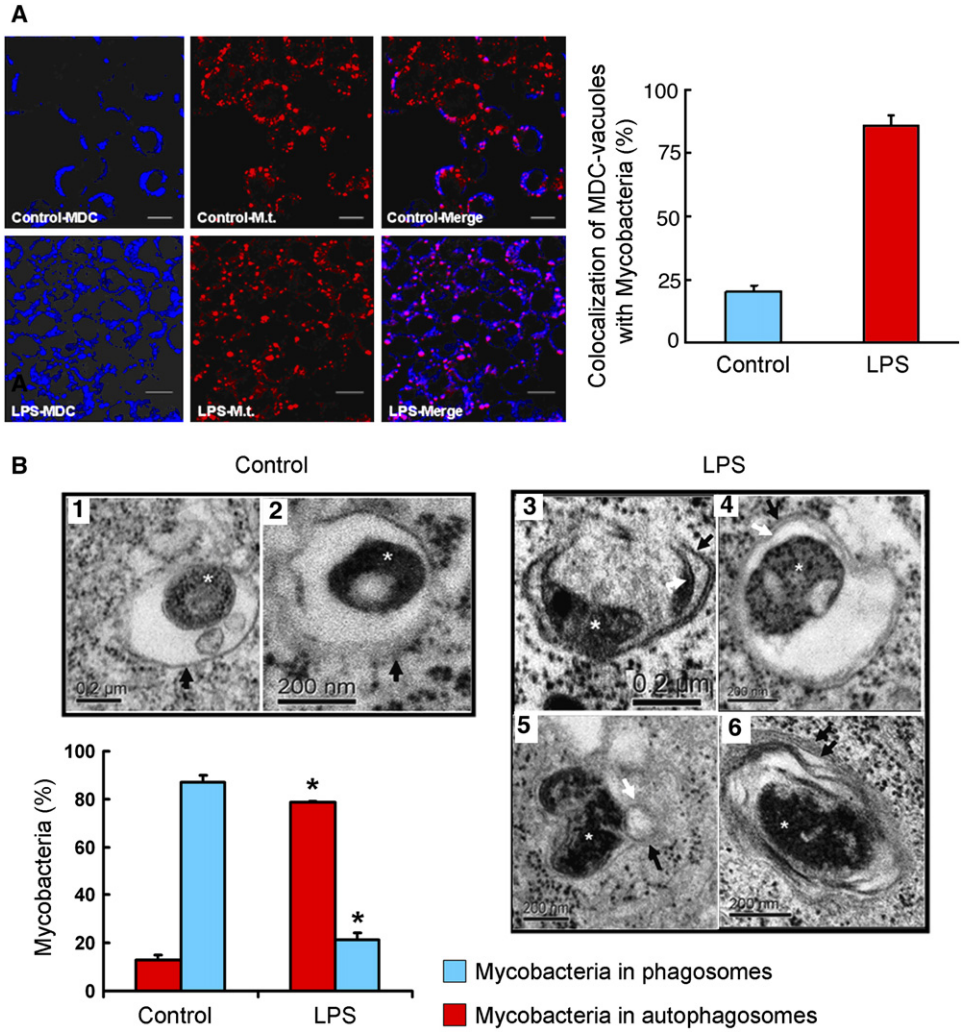

Figure 6. LPS-Induced Autophagy Promotes the Colocalization of Mycobacterial Phagosomes with the Autophagosomes

(A) RAW264.7 cells were infected with PKH26-stained *Mycobacterium tuberculosis* H37Rv (M.t., red) for 1 hr. After phagocytosis, cells were incubated in the presence or absence of LPS for 16 hr. Cells were fixed, and autophagic vacuoles were stained using MDC (blue). The colocalization of *M. tuberculosis* and the MDC-positive autophagosomes is represented in the merge panels by the pink color and quantitated in the graph at right (mean ± SEM, n = 2).

(B) Ultrastructural analysis of *M. tuberculosis* localization by transmission electron microscopy using RAW264.7 cells subjected to experiments as described in (A). In the absence of LPS (control), *M. tuberculosis* bacilli were found inside typical single-membrane mycobacterial phagosome compartments, indicated by black arrows in images 1 and 2. In contrast, in the presence of LPS, *M. tuberculosis* bacilli were found in typical double-membrane autophagosomes (images 3 and 4). Potential fusion events between mycobacterial phagosomes and autophagosomes were observed (image 5). Image 6 illustrates the presence of onion-like multilamellar structures containing mycobacteria. Black arrows, outer membranes; white arrows, internal membranes; double black arrows, onion-like multilamellar structures; white asterisks, *M. tuberculosis*. The graph represents the quantitation of 100 internalized mycobacteria per experimental condition (mean ± SD, n = 2; *p < 0.05).

colocalization of *M. tuberculosis* with GFP-LC3-positive autophagosomes. p38 MAPK inhibition, however, blocked LPS-induced colocalization of mycobacterial phagosomes with the autophagosomes. These results provided additional functional evidence for involvement of the p38 MAPK pathway in LPS-induced autophagy. Recent reports suggest that LRG47 exerts its antimycobacterial action by enhancing autophagy (Gutierrez et al., 2004; Singh et al., 2006). We observed that LPS induced upregulation of LRG47 expression in RAW264.7 cells and that LPS-induced LRG47 was almost exclusively membrane bound (Figure S7). These results suggested that LPS facilitated autophagosome formation through upregulation of LRG47 and promoting its membrane incorporation.

DISCUSSION

Although progress has been made in understanding the molecular mechanisms of starvation-induced autophagy, the signaling pathways leading to autophagy associated with innate immunity are not well studied. We studied autophagy in the murine macrophage cell line RAW264.7

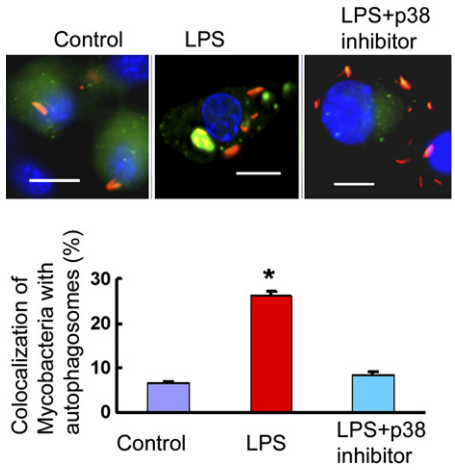

Figure 7. p38 MAPK Inhibition Blocks LPS-Induced Colocalization of *Mycobacterium tuberculosis* with Autophagosomes

RAW264.7 cells stably expressing GFP-LC3 were infected with *M. tuberculosis* expressing red fluorescent protein 1 hr prior to a 30 min incubation with p38 MAPK inhibitor or vehicle (DMSO) followed by further incubation for 16 hr in the presence or absence of LPS. Upper panel: representative fluorescence images. Lower panel: quantitation of percentage of colocalization of *M. tuberculosis* with GFP-LC3-positive autophagosomes. Graph represents the quantitation of 100 internalized mycobacteria per experimental condition. Data denote mean ± SEM from two independent experiments. *$p < 0.05$ versus control conditions. Scale bars = 10 μm.

and in primary human alveolar macrophages. In this study, we showed that TLR4 served as a previously unrecognized environmental sensor for autophagy. Autophagy was regulated through a TRIF-dependent, MyD88-independent TLR4 signaling pathway. RIP1 and p38 MAPK were downstream components of this pathway. This signaling pathway did not affect cell viability and was not mediated by JNK, indicating that it is distinct from the autophagic cell death signaling pathway. We further showed that LPS-induced autophagy could overcome mycobacterial phagosome arrest and force its colocalization with the autophagosomes.

There has been an intense controversy regarding the role of autophagy as a prosurvival or prodeath mechanism. Whereas inhibition of apoptosis enhances autophagic cell death (Yu et al., 2004), autophagy is essential for restricting cell death to infected sites in plants (Liu et al., 2005). The majority of evidence (Levine and Yuan, 2005) suggests that, in cells with intact apoptotic machinery and particularly in the context of innate immunity, autophagy is primarily a prosurvival pathway. Our study provides the molecular mechanisms for such a role. The JNK pathway has been shown to mediate RIP-induced autophagic cell death following caspase-8 inhibition (Yu et al., 2004). In our experiments, performed without caspase inhibition, LPS-induced autophagy had no effect on cell viability. The above results suggest that the signaling pathway for autophagy through RIP1 may undergo bifurcation downstream of RIP1. In the absence of caspase inhibition, RIP1 signaling is mediated through p38 MAPK and maintains cell survival. Under conditions favoring autophagic cell death, e.g., after caspase inhibition, RIP1 signaling is mediated through JNK, as previously shown (Yu et al., 2004). Thus, our data suggest that RIP1 acts as a critical mediator for autophagy in innate immunity and in controlling cell survival and death.

It is intriguing to note that among all TLRs, only TLR4 uses both the MyD88-dependent and MyD88-independent pathways. It had been unclear why both pathways are necessary. Our discovery of TRIF-dependent induction of autophagy may offer a mechanistic rationale for the need for two TLR4-mediated pathways. A plausible explanation could be that a close cooperation between the two arms for TLR4 is needed for innate immunity. For a mammalian cell to control a pathogen, two processes will need to be performed in sequence: phagocytosis for pathogen internalization, and then autophagy, which would involve fusion of the phagosome with autophagosome, which matures and fuses with lysosomes. A previous study suggested that the TLR4-MyD88-dependent pathway is needed for phagocytosis (Blander and Medzhitov, 2004). Phagocytosis of the Gram-negative bacteria *E. coli* is impaired in MyD88-deficient cells. A cooperation model would suggest that TLR4-MyD88, a fast-response pathway, would be in charge of phagocytosis and that TLR4-TRIF, a slower-response pathway, would be in charge of autophagy.

In macrophages infected with *M. tuberculosis*, induction of autophagy by LPS had a marked effect on overcoming *M. tuberculosis* phagosome block and promoting its colocalization with autophagosome. *M. tuberculosis* does not have LPS in its wall and does not directly activate TLR4. Activation of autophagy by stimulating the TRIF pathway may offer an unexpected therapeutic approach against *M. tuberculosis*. Our study unravels an important aspect of autophagy regulation and provides a link between stimulation of autophagy and pattern recognition receptors of innate immunity. Thus, it opens a new window for potential therapeutic interventions for modulation of autophagy through the TLRs. These new therapeutic strategies might be able to outsmart pathogens, some of which rely on suppressing autophagy for their survival.

EXPERIMENTAL PROCEDURES

Cell and Bacterial Cultures

RAW264.7 cells were maintained in Dulbecco's modified Eagle's medium containing 10% fetal bovine serum. *Mycobacterium tuberculosis* H37Rv was grown in Middlebrook 7H9 broth medium supplemented with 0.2% glycerol and 0.25% Tween 80 or on 7H11 agar plates and homogenized to generate a single cell suspension. In some experiments, *M. tuberculosis* was stained with 10% PKH26 red fluorescent dye (Sigma) according to the manufacturer's instructions. Primary human macrophages were from bronchoalveolar lavage (BAL) fluid of subjects undergoing a medically indicated bronchoscopy for a localized pulmonary nodule. BAL was performed before diagnostic evaluation of pulmonary lesion, and BAL fluid was obtained from either right middle or lingual lobe. The research protocol was approved by institutional review board of Baylor College of Medicine.

Antibodies and Reagents

LC3 antibody used for immunoblot was purchased from ANASpec, LC3 antibody used for immunofluorescence was a gift from Takashi Ueno, MyD88 antibody was from Stressgen, TRIF antibody was from Abcam, LAMP1 antibody was from ABR, VPS34 antibody was from Invitrogen, LRG47 antibody was from Santa Cruz, and iNOS antibody was from Research & Diagnostic Antibodies. LC3A cDNA was cloned from human brain RNA and subcloned into the C-terminal end of enhanced GFP (BD Biosciences) to produce GFP-LC3. Mouse MyD88-DN plasmid was from InvivoGen. TLR4-DN (P712H) plasmid was a gift from Sankar Ghosh. Human VPS34-DN (N743A-N748I) plasmid was a gift from Robert Moore. LPS of *Escherichia coli* serotype 0111:B4, 3MA, wortmannin, and PKH26 red fluorescent dye were from Sigma. p38 MAPK inhibitor (SB 203580) and JNK inhibitor II were from Calbiochem.

Transfection and Establishment of Stable Cell Lines

RAW264.7 cells were transfected by electroporation using program D-32 of an Amaxa Nucleofector (Amaxa). RAW264.7 cells stably expressing GFP-LC3 or VPS34 were selected and maintained in G418. A stable cell line clone expressing both GFP-LC3 and a MyD88-DN mutant was selected and maintained in the presence of both G418 (600 μg/ml) and Zeocin (50 μg/ml).

Cell Lysis and Fractionation

Cells were lysed on ice for 30 min in 40 mM Bis-Tris propane buffer (pH 7.7), 150 mM NaCl, 10% glycerol, 1% Triton X-100, and protease inhibitors. Fractionation of cellular proteins into cytosolic soluble and membrane particulate fractions was performed as follows. Cells were homogenized with a sonicator, and lysates were ultracentrifuged for 30 min at 100,000 × g at 4°C. The supernatant was removed (soluble fraction), and the remaining pellet was subjected to a second round of sonication and ultracentrifugation as above. The final pellet was resuspended in phosphate-buffered saline (particulate fraction).

Autophagy Assays

Autophagy was evaluated in cells by fluorescence microscopy, EM, or immunoblot. In fluorescence microscopy experiments, autophagy was evaluated by examining the punctate forms (type II) of the autophagy marker LC3. Experiments studied either GFP-LC3 or endogenous LC3 stained by LC3 antibody. Quantitation of autophagy was performed based on the percentage of GFP-LC3-positive autophagic vacuoles or cells with LC3 punctate dots. In some experiments, autophagy was evaluated by observing the MDC-positive autophagic vacuoles. In EM experiments, autophagy was evaluated by observing the typical double-membrane vesicles (Ogawa et al., 2005; Gutierrez et al., 2004; Liu et al., 2005). In experiments using EM, autophagy was quantitated by determining the number of autophagic vacuoles per cross-sectioned cell. In all experiments, a minimum of 100 cells per sample were counted, and duplicate or triplicate samples were counted per experimental condition. For EM experiments, data obtained from a minimum of 50 independent sectioned cells were used. Statistical analysis was performed using a two-tailed Student's t test (Liu et al., 2005).

Fluorescence Microscopy

Cells were grown on collagen-precoated glass coverslips in six-well plates. Cells were fixed with 4% paraformaldehyde, mounted using the SlowFade Antifade Kit (Invitrogen) and the blue nuclear chromatin stain 4′,6-diamidino-2-phenylindole dihydrochloride (DAPI), and viewed using a Zeiss Axiovert 200M microscope. Z sections were collected at an optical depth of 0.2–0.8 μm, and images were optimized with deconvolution software. In immunofluorescence experiments, following fixation, cells were permeabilized with 0.2% Triton X-100, blocked with 10% normal goat serum, and incubated with primary antibodies followed by secondary antibodies before mounting (Kolodziejska et al., 2005).

RNA Interference

siRNAs against TLR4 were from the SureSilencing Mouse TLR4 kit (SuperArray Bioscience Corporation). siRNAs designed against MyD88, TRIF, and RIP1 were from Dharmacon using the following sequences: MyD88, sense 5′-GCCUAUCGCUGUUCUUGAAUU-3′, antisense 5′-UUCAAGAACAGCGAUAGGC-3′; TRIF, sense 5′-GGAAAGCAGUGGCCUAUUA-3′, antisense 5′-UAAUAGGCCACUGCUUUCC-3′; RIP1, sense 5′-CCACUAGUCUGACUGAUGA-3′, antisense 5′-UCAUCAGUCAGACUAGUGG-3′. siRNAs were transiently transfected using Lipofectamine 2000 (Invitrogen). As a control, we used either siRNA against luciferase (Dharmacon) or gene-specific scrambled siRNA.

Transmission Electron Microscopy

RAW264.7 cells were fixed in 2.5% glutaraldehyde in 0.1 M sodium cacodylate buffer (pH 7.0) for 1 hr, postfixed in 1% osmium tetroxide in 0.1 M cacodylate buffer for 1 hr, dehydrated with increasing concentrations of ethanol, and gradually infiltrated with Araldite resin. Ultrathin sections (70–80 nm) were obtained using an ultramicrotome (RMC MT6000-XL). Sections were stained with uranyl acetate and lead citrate and examined using a Hitachi H-7500 transmission electron microscope equipped with a Gatan digital camera.

Functional Assays of JNK and p38 MAPK Inhibitors

Functional assays of JNK and p38 MAPK inhibitors were performed by assaying the phosphorylation of the downstream targets of JNK and p38 MAPK in RAW264.7 cells incubated in the presence or absence of the corresponding inhibitors. JNK activity was assayed by analyzing phosphorylation of Ser63 of c-Jun. p38 MAPK activity was assayed by evaluating phosphorylation of Thr334 of MAP kinase-activated protein kinase 2. MAP kinase-activated protein kinase 2 is a downstream target of p38 MAPK (Zarubin and Han, 2005) and c-Jun is a downstream target of JNK (Holzberg et al., 2003).

Supplemental Data

Seven figures are available at http://www.immunity.com/cgi/content/full/27/1/135/DC1/.

ACKNOWLEDGMENTS

This work was supported by NHLBI, NIAID, AHA, and the Alpha-1 Foundation to N.T.E. and by NIH Kirschstein National Research Service Award 1F32 HL078520-01 to Y.X. We thank providers of plasmids and reagents as detailed throughout the text and Margie Moczygemba and Li-Yuan Yu-Lee for critical review of the manuscript.

Received: January 8, 2007
Revised: April 11, 2007
Accepted: May 8, 2007
Published online: July 19, 2007

REFERENCES

Beutler, B., and Rietschel, E.T. (2003). Innate immune sensing and its roots: the story of endotoxin. Nat. Rev. Immunol. *3*, 169–176.

Blander, J.M., and Medzhitov, R. (2004). Regulation of phagosome maturation by signals from toll-like receptors. Science *304*, 1014–1018.

Devin, A., Lin, Y., and Liu, Z.G. (2003). The role of the death-domain kinase RIP in tumour-necrosis-factor-induced activation of mitogen-activated protein kinases. EMBO Rep. *4*, 623–627.

Duff, G.W., and Atkins, E. (1982). The inhibitory effect of polymyxin B on endotoxin-induced endogenous pyrogen production. J. Immunol. Methods *52*, 333–340.

Gutierrez, M.G., Master, S.S., Singh, S.B., Taylor, G.A., Colombo, M.L., and Deretic, V. (2004). Autophagy is a defense mechanism inhibiting BCG and Mycobacterium tuberculosis survival in infected macrophages. Cell *119*, 753–766.

Holzberg, D., Knight, C.G., Dittrich-Breiholz, O., Schneider, H., Dorrie, A., Hoffmann, E., Resch, K., and Kracht, M. (2003). Disruption of the c-JUN-JNK complex by a cell-permeable peptide containing the c-JUN delta domain induces apoptosis and affects a distinct set of interleukin-1-induced inflammatory genes. J. Biol. Chem. *278*, 40213–40223.

Holler, N., Zaru, R., Micheau, O., Thome, M., Attinger, A., Valitutti, S., Bodmer, J.L., Schneider, P., Seed, B., and Tschopp, J. (2000). Fas triggers an alternative, caspase-8-independent cell death pathway using the kinase RIP as effector molecule. Nat. Immunol. *1*, 489–495.

Kawai, T., and Akira, S. (2005). Toll-like receptor downstream signaling. Arthritis Res. Ther. *7*, 12–19.

Kihara, A., Noda, T., Ishihara, N., and Ohsumi, Y. (2001). Two distinct Vps34 phosphatidylinositol 3-kinase complexes function in autophagy and carboxypeptidase Y sorting in Saccharomyces cerevisiae. J. Cell Biol. *152*, 519–530.

Kirkegaard, K., Taylor, M.P., and Jackson, W.T. (2004). Cellular Autophagy: surrender, avoidance and subversion by microorganisms. Nat. Rev. Microbiol. *2*, 301–314.

Kolodziejska, K.E., Burns, A.R., Moore, R.H., Stenoien, D.L., and Eissa, N.T. (2005). Regulation of Inducible Nitric Oxide Synthase by Aggresome Formation. Proc. Natl. Acad. Sci. USA *102*, 4854–4859.

Levine, B., and Klionsky, D.J. (2004). Development by self-digestion: molecular mechanisms and biological functions of autophagy. Dev. Cell *6*, 463–477.

Levine, B. (2005). Eating oneself and uninvited guest: autophagy-related pathways in cellular defense. Cell *120*, 159–162.

Levine, B., and Yuan, J. (2005). Autophagy in cell death: an innocent convict? J. Clin. Invest. *115*, 2679–2688.

Liu, Y., Schiff, M., Czymmek, K., Talloczy, Z., Levine, B., and Dinesh-Kumar, S.P. (2005). Autophagy regulates programmed cell death during the plant innate immune response. Cell *121*, 567–577.

Lorenz, E., Patel, D.D., Hartung, T., and Schwartz, D.A. (2002). Toll-like receptor 4 (TLR4)-deficient murine macrophage cell line as an in vitro assay system to show TLR4-independent signaling of Bacteroides fragilis lipopolysaccharide. Infect. Immun. *70*, 4892–4896.

Lum, J.J., Bauer, D.E., Kong, M., Harris, M.H., Li, C., Lindsten, T., and Thompson, C.B. (2005). Growth factor regulation of autophagy and cell survival in the absence of apoptosis. Cell *120*, 237–248.

MacMicking, J.D., Taylor, G.A., and Mickinney, J.D. (2003). Immune control of tuberculosis by IFN-γ-inducible LRG-47. Science *302*, 654–659.

Meylan, E., Burns, K., Hofmann, K., Blancheteau, V., Martinon, F., Kelliher, M., and Tschopp, J. (2004). RIP1 is an essential mediator of Toll-like receptor 3-induced NF-kappa B activation. Nat. Immunol. *5*, 503–507.

Musial, A., and Eissa, N.T. (2001). Inducible nitric oxide synthase is regulated by the proteasome degradation pathway. J. Biol. Chem. *276*, 24268–24273.

Nakagawa, I., Amano, A., Mizushima, N., Yamamoto, A., Yamaguchi, H., Kamimoto, T., Nara, A., Funao, J., Nakata, M., Tsuda, K., et al. (2004). Autophagy defends cells against invading group A *Streptococcus*. Science *306*, 1037–1040.

Ogawa, M., Yoshimori, T., Suzuki, T., Sagara, H., Mizushima, N., and Sasakawa, C. (2005). Escape of intracellular *Shigella* from autophagy. Science *307*, 727–731.

Palsson-McDermott, E.M., and O'Neill, L.A. (2004). Signal transduction by the lipopolysaccharide receptor, Toll-like receptor-4. Immunology *113*, 153–162.

Seglen, P.O., and Gordon, P.B. (1982). 3-Methyladenine: specific inhibitor of autophagic/lysosomal protein degradation in isolated rat hepatocytes. Proc. Natl. Acad. Sci. USA *79*, 1889–1892.

Singh, S.B., Davis, A.S., Taylor, G.A., and Deretic, V. (2006). Human IRGM induces autophagy to eliminate intracellular mycobacteria. Science *313*, 1438–1441.

Stein, M.P., Feng, Y., Cooper, K.L., Welford, A.M., and Wandinger-Ness, A. (2003). Human VPS34 and p150 are Rab7 interacting partners. Traffic *4*, 754–771.

Takeda, K., and Akira, S. (2005). Toll-like receptors in innate immunity. Int. Immunol. *17*, 1–14.

Xu, Y., Kim, S.O., Li, Y., and Han, J. (2006). Autophagy contributes to caspase-independent macrophage cell death. J. Biol. Chem. *281*, 8788–8795.

Yu, L., Alva, A., Su, H., Dutt, P., Freundt, E., Welsh, S., Baehrecke, E.H., and Lenardo, M.J. (2004). Regulation of an ATG7-beclin1 program of autophagic cell death by caspase-8. Science *304*, 1500–1502.

Zarubin, T., and Han, J. (2005). Activation and signaling of the p38 MAP kinase pathway. Cell Res. *15*, 11–18.